

Nuclear Magnetic Resonance: Spin-Spin and Spin-Lattice Relaxation Times

Adrian Thompson

Physics 134 Advanced Laboratory

Lab Partner: Oscar Flores

University of California, Santa Cruz

May 18, 2014

Abstract

The fundamentals of pulsed nuclear magnetic resonance (PNMR) were investigated in a series of experiments using a sample of mineral oil, a benchtop magnet, and a radio frequency (RF) pulse programmer. The apparatus was set up to observe a free induction decay (FID) signal response in the sample magnetization and measure the homogeneity in the static magnetic field contour. The spin-lattice (T_1) and spin-spin (T_2) relaxation times of the sample were measured to be 7.48 ± 0.39 ms and 22.69 ± 0.82 ms, respectively.

1 Introduction

Pulsed nuclear magnetic resonance (NMR) has many applications in modern science, with some examples being the medical imaging of biological systems or spectroscopy in organic and inorganic chemistry. In these experiments we focus on the core principles of spin-spin and spin-lattice relaxation times, which are characteristic time scales during non-equilibrium conditions imposed on materials by external fields. We used a sample of mineral oil as a material, and a benchtop NMR magnet and pulse programmer to observe the aforementioned phenomena. These apparatus are discussed in further detail in section 2.

1.1 The Resonance Condition and Larmor Precession

The following discussion can be found in [5]. Please see [6] as well.

Protons have spin angular momentum and an associated magnetic moment, and their response to external magnetic fields is an increasingly valuable phenomenon in modern applications. The spin vector $\mathbf{S} = \hbar\mathbf{l}$ and the magnetic moment vector $\boldsymbol{\mu}$ are aligned and related by a proportionality constant called the gyromagnetic ratio;

$$\boldsymbol{\mu} = \gamma\mathbf{S} \tag{1}$$

$$\boldsymbol{\mu} = \gamma\hbar\mathbf{l} \tag{2}$$

In an external, uniform magnetic field, the energy of these dipoles is given by

$$E = -\boldsymbol{\mu} \cdot \mathbf{B}_{\text{ext}} \tag{3}$$

Taking the uniform field in a coordinate system (x, y, z) as $\mathbf{B} = B_0\hat{\mathbf{z}}$, we evaluate the energy by combining the above equations.

$$\begin{aligned} E &= -\mu_z B_0 \\ &= -\gamma\hbar l_z B_0 \end{aligned}$$

For fermions, $l_z = \pm \frac{1}{2}$ and therefore the energy spacing between these two states is

$$\begin{aligned} \Delta E &= |E_{\frac{1}{2}} - E_{-\frac{1}{2}}| \\ &= \left| -\gamma\hbar\left(\frac{1}{2}\right)B_0 + \gamma\hbar\left(-\frac{1}{2}\right)B_0 \right| \\ &= \gamma\hbar B_0 \end{aligned}$$

The quantum mechanical treatment allows the expression of this energy difference as $\Delta E = \hbar\omega_0$, so

$$\omega_0 = \gamma B_0. \quad (4)$$

The frequency ω_0 is known as the Larmor precession frequency. Larmor precession is the classical mechanical notion of the precession of the angular momentum vector \mathbf{J} precessing about an applied magnetic field \mathbf{B} . Classically, $\omega_0 = \frac{qB}{2m}$ for a charge q . However, a quantum mechanical treatment must include the “ g -factor” with g not necessarily 1;

$$\omega_0 = \frac{qgB}{2m}$$

giving

$$\gamma = \frac{qg}{2m}.$$

Quantum mechanically, ω_0 is a photon frequency associated with the change of energy states from $l_z = \frac{1}{2}$ (parallel) to $l_z = -\frac{1}{2}$ (antiparallel).

1.2 Relaxation Times

With an external field $\mathbf{B} = B_0\hat{\mathbf{z}}$ causing the precession of all the magnetic moments $\boldsymbol{\mu}_i$ in a sample volume, we can define a net magnetization:

$$\mathbf{M} = \sum_{i=1}^N \boldsymbol{\mu}_i. \quad (5)$$

As \mathbf{B} is applied, random variations in the sample cause dephasing in the Larmor precessions on the magnetic moments. When thermal equilibrium is attained, a symmetry in the precession phases is extant such that there is no net magnetization in the xy plane. If we pulse a transverse magnetic field (TM field) in the xy plane, the magnetic moments (spins) in the sample get offset by an angle away from the $\hat{\mathbf{z}}$ direction.

There are two relaxation processes that can be observed during this non-equilibrium condition. Firstly, the spins in the sample will return to their equilibrium precession about $B_0\hat{\mathbf{z}}$; secondly, the pulse will bring all of the moments into phase with each other, thus breaking the phase symmetry, and they will take time to dephase again. These processes relax to equilibrium exponentially, each with characteristic time constants. The former process has a time constant called the “spin-lattice” relaxation time (T_1) and the latter has a time constant called the “spin-spin” relaxation

time (T_2). These times contain some information about how a material's molecular or atomic constituents communicate electronically with neighboring atoms and molecules in the "lattice" (spin-lattice) and the interaction between spins in a given molecule (spin-spin). In spin-lattice, the nuclei are returning to their equilibrium precession while returning energy to the lattice thermally. Here, the word "lattice" is used loosely to mean the isotropic environment surrounding any constituent, like a molecule, in the material.

2 Methods

2.1 Apparatus and Procedure

The full apparatus schematic is shown in figure 1. The devices we used are detailed below in figures 2, 3, and 4.

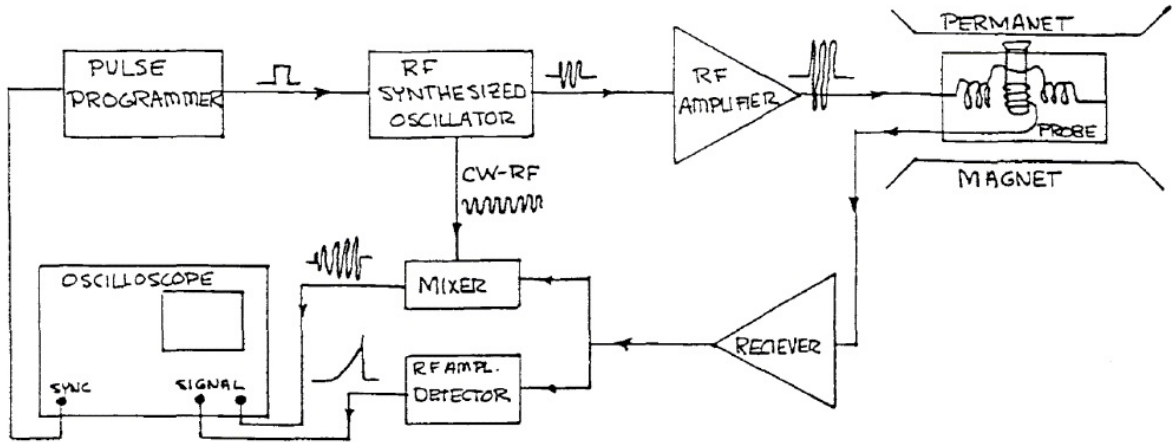


Figure 1: The block diagram for the device chain used to send pulses and mix the FID and echo signals with the pulsed frequency [3].



Figure 2: The TeachSpin PM 1501 magnet.

The magnet shown in Figure 2 is capable of applying static and pulsed fields. A sample can be inserted into a vertical capsule in the center of the device. Permanent magnets provide a static field, in what we labeled the z direction, across the sample. The sample is flanked by two Helmholtz coils, which provide the pulsed field out of or into the plane of the chassis face, perpendicular to the static field. The knobs on the side and front of the magnet can be used to adjust the sample position in the xy plane; we used this feature to find the most "flat" or homogeneous regime of the static field as a preliminary step to measuring pulse responses.

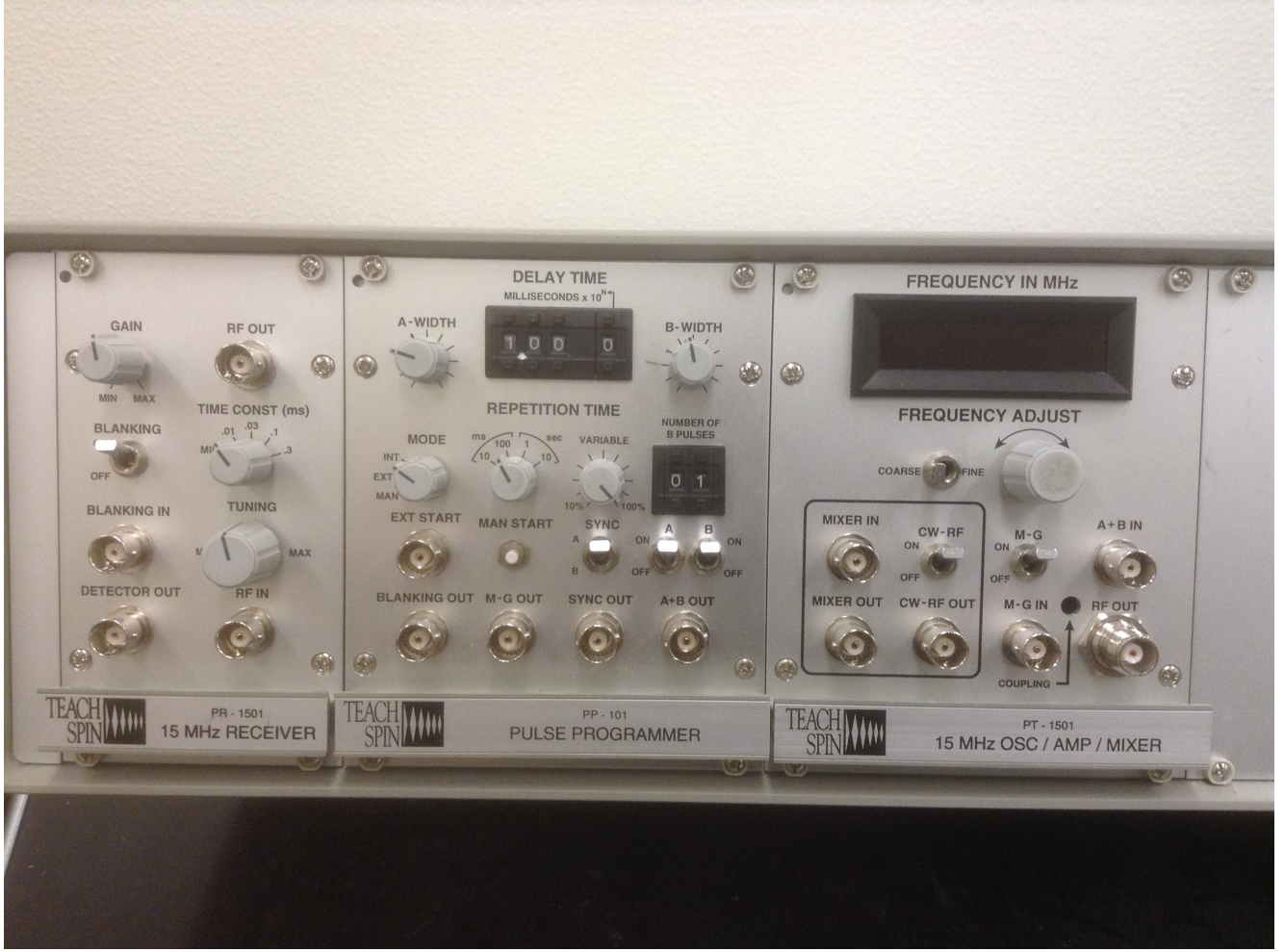


Figure 3: The TeachSpin pulse programmer.

The pulse programmer seen in figure 3 is what we used to control the pulse sequences. We controlled two pulse types via the “A” and “B” settings, which include control over the A and B width and the delay time τ between pulses A and B. We used the frequency adjust knob to sweep over the range of radio frequencies and find the resonance frequency in Hertz. As in figure 1, the CW (continuous wave) signal generated by the oscillator in the pulse programmer was set up to be mixed with the outgoing signal response from the magnetized sample. The mixed signal therefore had a beat frequency, which could be seen on the oscilloscope.

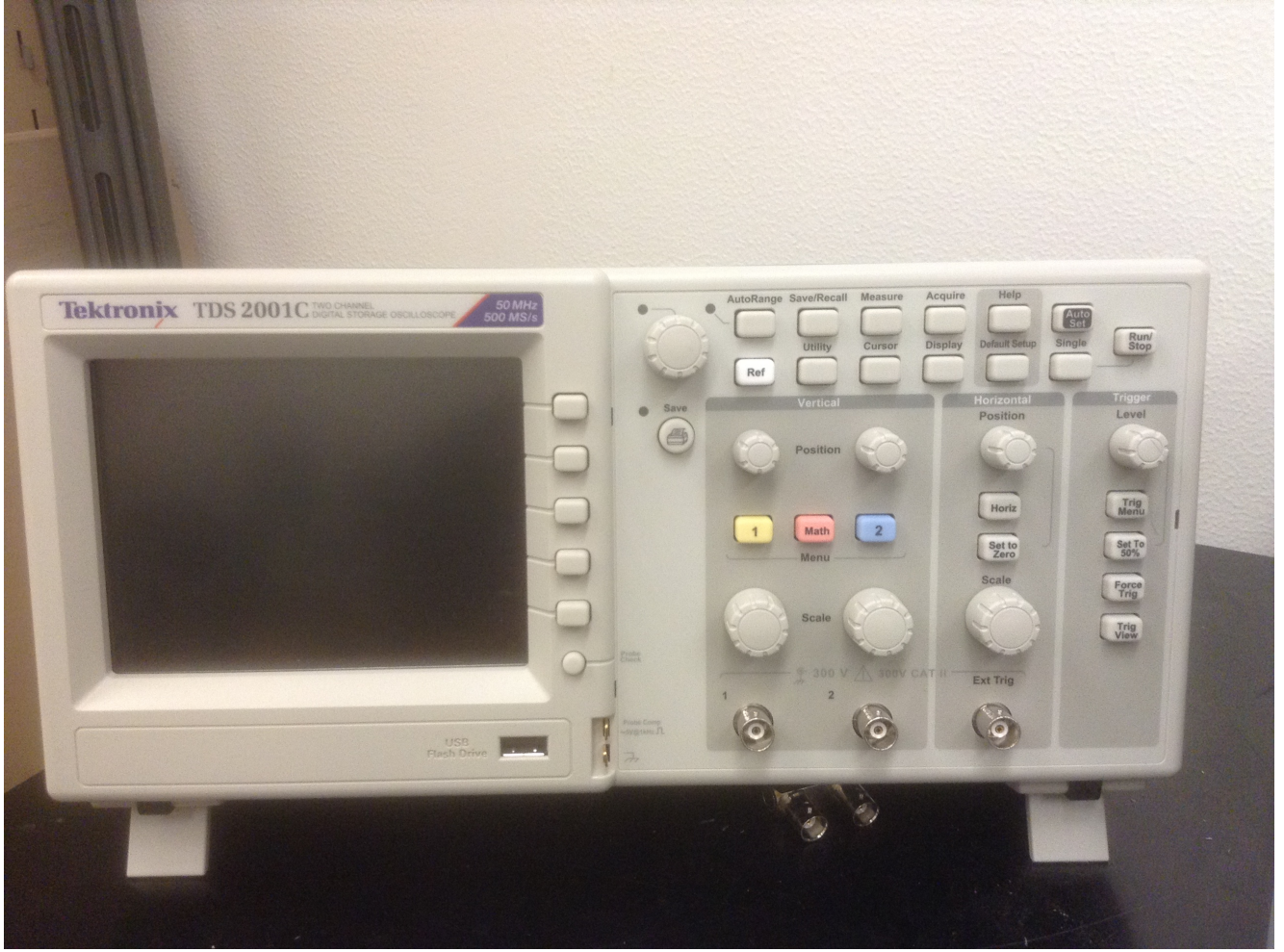


Figure 4: The Tektronix TDS 2001C digital oscilloscope.

The oscilloscope makes measurements of incoming voltages from the apparatus. These voltages are proportional to the magnetizations measured by the receiver coils, so we call voltage traces on the oscilloscope the relative magnetization.

2.2 Achieving Resonance

To match the frequency ω of the pulsed magnetic field B_1 to the resonance condition for ω_0 , we scanned across a range of frequencies in the radio frequency (RF) range on the pulser until the mixed signal no longer had a beat frequency. This was observed on the oscilloscope as a beat envelope flattening out as the resonance frequency was reached. The exponential decay envelope that followed this pulse is called the free induction decay signal (FID).

2.3 180° and 90° Pulses

To probe the different relaxation times, we made use of two types of pulses. These pulses can be made to rotate the magnetization of the sample by 180° or 90° away from the equilibrium magnetization. We can control how much these pulses rotate the magnetization by controlling the pulse width of the square wave before it reaches the oscillator (see Figure 1). To achieve a 90° pulse, the resonance condition must first be met so that the effective field is static in the rotating frame. We needed resonance to be sure that the magnetization was rotated into the xy plane; since the probe, which is a pickup or receiver coil, has its axis oriented in the z -direction and only feels xy EMF's, its maximum induced EMF occurs during a total xy magnetization of the sample (90°). Once we matched the resonance frequency, we looked for the maximum amplitude

in the free induction decay signal; this was the sign of a true 90° pulse.

For a 180° pulse, we expected no FID tail. This is because a 180° pulse rotates the magnetization to an unstable equilibrium position through the transformation $M_z \rightarrow -M_z$. In truth, each of the nucleon spins have x and y components along their precession, but phase symmetry across the sample destructively interferes to produce only a net M_z (use equation 5 setting $\sum_{i=1}^N \mu_x = 0$, $\sum_{i=1}^N \mu_y = 0$). Since the pickup coils in the magnet probe do not pickup any \hat{z} magnetization, no signal can be observed as \mathbf{M} is constrained to the z axis during its return to equilibrium. To obtain this, we varied the duration (or width) of the square wave until the FID tail was minimal on the oscilloscope screen.

2.4 Spin-Lattice Relaxation Time T_1

$$M(t) = M_0(1 - e^{-\frac{t}{T_1}}) \quad (6)$$

Equation 6 describes the magnetization's exponential growth toward equilibrium. T_1 is the spin-lattice relaxation time. Notice that as $t \rightarrow \infty$, the magnetization returns to equilibrium. What is observed in the lab is actually an exponential decay from the pickup coils measuring diminishing xy magnetization. Therefore, the equation that models our oscilloscope FID signal trace is

$$M(t) = M_0 e^{-\frac{t}{T_1}} \quad (7)$$

To obtain an approximation of T_1 , we sent a 90° pulse to rotate the spins of the sample into the xy plane. We observed the FID pulse on the oscilloscope and We used a 180° pulse followed by a 90° pulse and plotted the height of the FID signal from the 90° pulse as a function of the delay time τ .

2.5 Spin-Spin Relaxation Time T_2

The spin-spin relaxation time T_2 , like T_1 , also satisfies a decaying exponential, but this time only in the x and y directions. The full magnetization equation as a function of t for T_2 is

$$M(t) = M_0 e^{-\frac{1}{6}(\frac{t}{T_2})^3} \quad (8)$$

(see [1]). Since our apparatus does not measure z magnetization, the actual relationship we looked for is given in equation 9, found in [3]:

$$M_{x,y}(t) = M_0 e^{-\frac{t}{T_2}} \quad (9)$$

The spin-lattice and spin-spin relaxations are happening simultaneously as the sample magnetization is displaced from equilibrium. The way we separated the two phenomena into two observables was by a M-G (Meiboom-Gill) series of pulses, based on the Carr-Purcell method [2]. Explicitly, we used a 90° pulse followed by a 180° pulse. This is the Carr-Purcell method described in pages 34-35 of [3] or in [2]. The 90° pulse rotates the moments μ_i into the xy plane; they will be undergoing FID, but their precessions will also be dephasing back to a symmetric magnetization. Before their FID finishes (i.e. before T_1), a 180° pulse displaces the moments to precess in the opposite direction, still in the xy plane. This allows the moments to completely rephase while in the xy plane, decoupled from their normal FID paths. The moment that they rephase incurs a maximum readout voltage in the pickup coil, which can be seen on the oscilloscope as a "hump" ;

this is called a spin-echo signal. The delay time, τ , between the two pulses is the same as the delay time between the second pulse and the spin-echo. We then plotted the spin-echo pulse height as a function of twice the delay time, 2τ . This extracted T_2 for us without simultaneously measuring T_1 [3];

$$M(2\tau) = M_0 e^{-\frac{2\tau}{T_2}} \quad (10)$$

We used a modified version of the Carr-Purcell method called the Meiboom-Gill or M-G method. Everything remains mathematically the same, but a phase-shift technique during the pulse sequence ensures that a true 180° pulse has been achieved [4]. This technique was used by simply turning on the “M-G” switch on the pulse programmer.

2.6 Errors and Data Software

We used an estimation method to determine the errors made on the relative magnetization measured by the oscilloscope trace. We used the cursor function on the oscilloscope to measure these heights; since the trace was quite noisy (see figures 6 and 8), we took the error on the trace to be half the width of the trace. We approximated half the width to be 0.07 Volts, so we took $\sigma_{M(t)}$ for both T_1 and T_2 measurements to be ± 0.07 .

The data collected was fit using Gnuplot’s Levenberg-Marquardt algorithm, which determined for us a reduced Chi-Squared (χ^2) value. We could easily obtain the true χ^2 after multiplying by the degrees of freedom ν . We then used an online chi-squared calculator [7] to obtain a confidence value α from the χ^2 value (this is the error function result $\text{erf}(\chi^2, \nu)$; see [7] for the exact formula).

3 Results

3.1 Magnetic Field Homogeneity

We first needed to determine a linear regime to place our sample. We plotted the FID height as a function of the sample’s position in the yz plane (moving in y , perpendicular to the static field and parallel to the pulse direction. The flattest part of the curve, in the neighborhood of -1.5 cm, is where we decided the most homogeneous part of the field was. We used that position to setup our pulses for the following parts of the experiment.

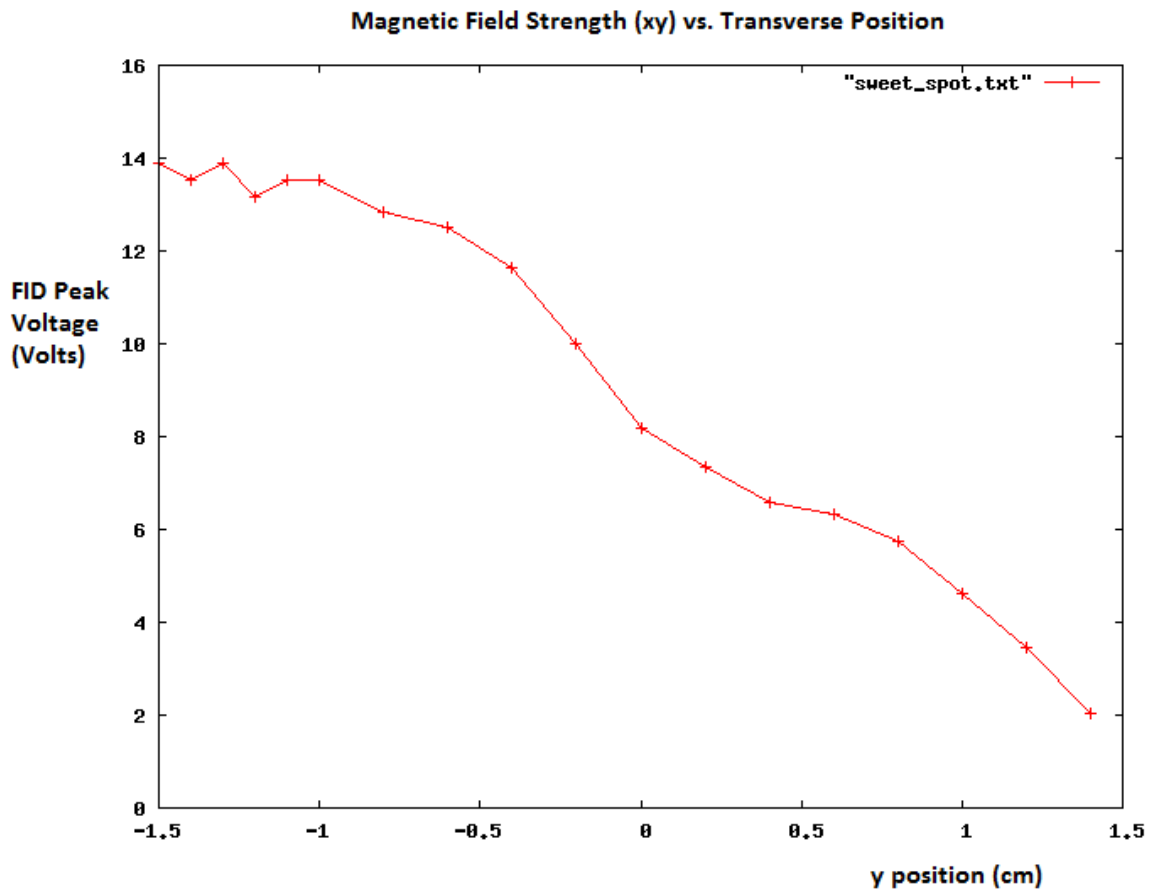


Figure 5: The flat regions are associated with linear or homogeneous regimes of the static magnetic field contour.

3.2 Resonance Condition

We used the method discussed in section 2.2 to find the resonance frequency. We found it to vary between 15.46200 MHz and 15.45800 MHz, with an average of 15.45967 ± 0.0017 MHz. We believe that these variations originate from temperature variations in the magnet.

$$\omega_0 = 15.45967 \pm 0.0017 \text{ MHz}$$

3.3 Spin-Lattice Relaxation Time T_1

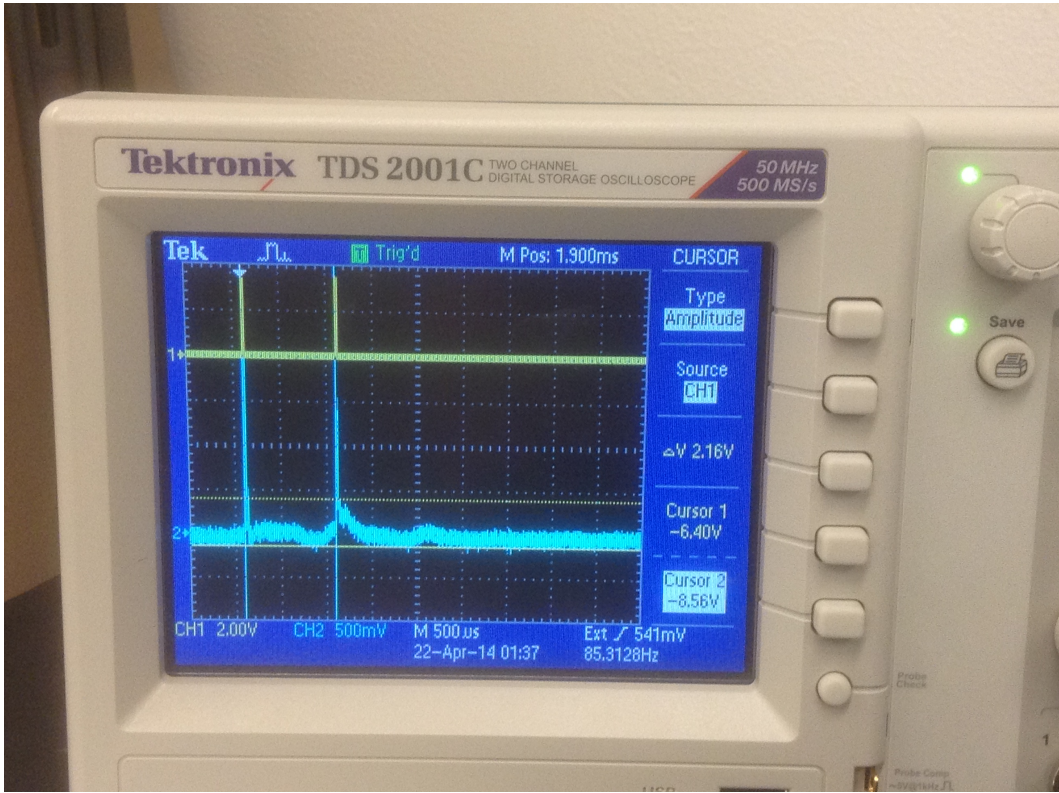


Figure 6: The oscilloscope trace for measuring the spin-lattice time T_1 .

We plotted $M(\tau)$. The magnetization is proportional to the voltage read by the pickup coils and eventually transmitted through to the oscilloscope. The actual voltage we are reading is the height of the FID signals. We extract the best fit using an exponential functional form $a \cdot e^{-\frac{\tau}{b}}$ using Gnuplot's Marquardt algorithm and took $b = T_1$. See figure 7.

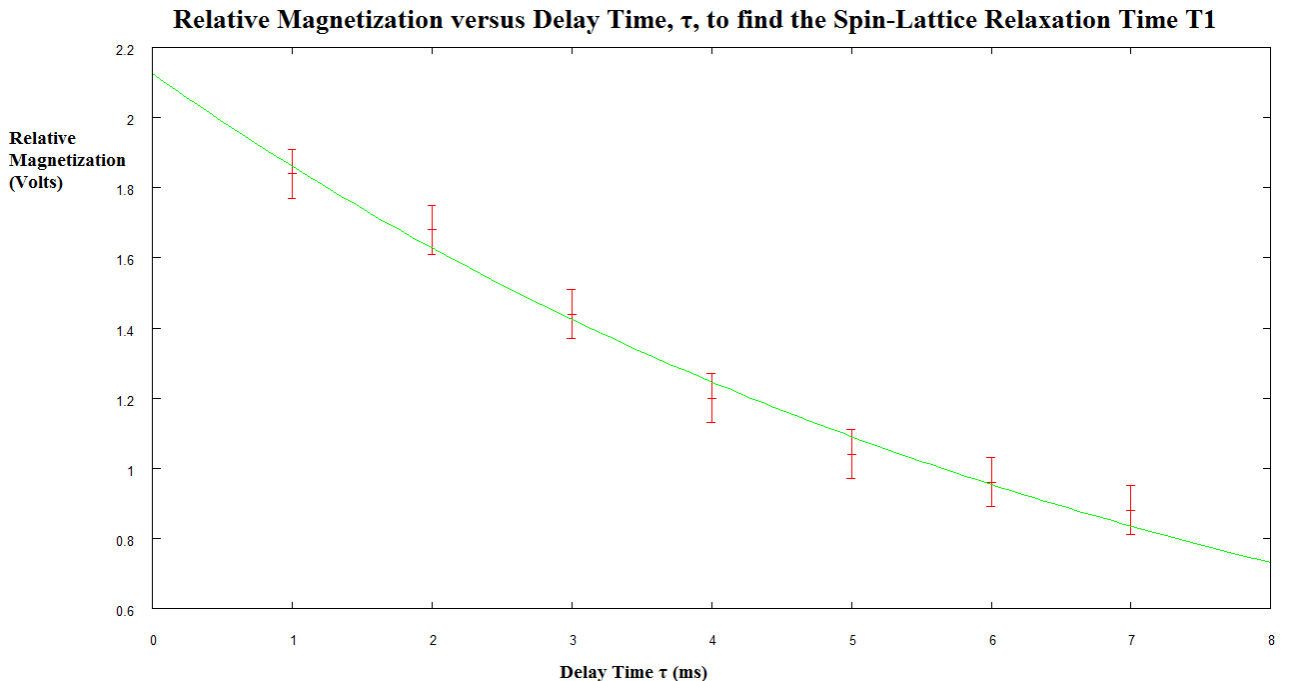


Figure 7

$$\begin{aligned}
T_1 &= 7.48 \pm 0.39 \text{ ms} \\
\text{Degrees of Freedom} &\quad \nu = 5 \\
&\quad \chi^2 = 2.0696 \\
\text{Confidence Value} &\quad \alpha = 0.8394
\end{aligned}$$

3.4 Spin-Spin Relaxation Time T_2

Again we plotted the magnetization, but this time as a function of 2τ . We used the same fitting process as in section 3.2 to produce the best fit and T_2 using an exponential functional form. See figure 9.

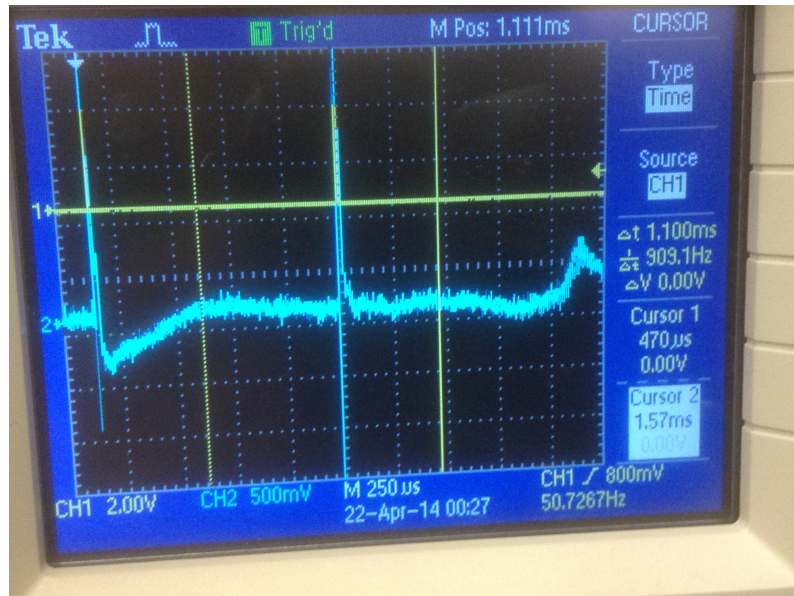


Figure 8: The M-G pulse train for measuring T_2 . The spin-echo hump is visible on the right of the oscilloscope screen.

Here, χ^2 is the unreduced Chi-Squared of the fit, and α is the confidence value, or the error function result of the Chi-Squared distribution integrating from χ^2 . For this measurement and for the measurement of T_2 , we used errors of 0.2 Volts for each data point. We draw this measurement from the thickness of the oscilloscope trace, seen in figure 8.

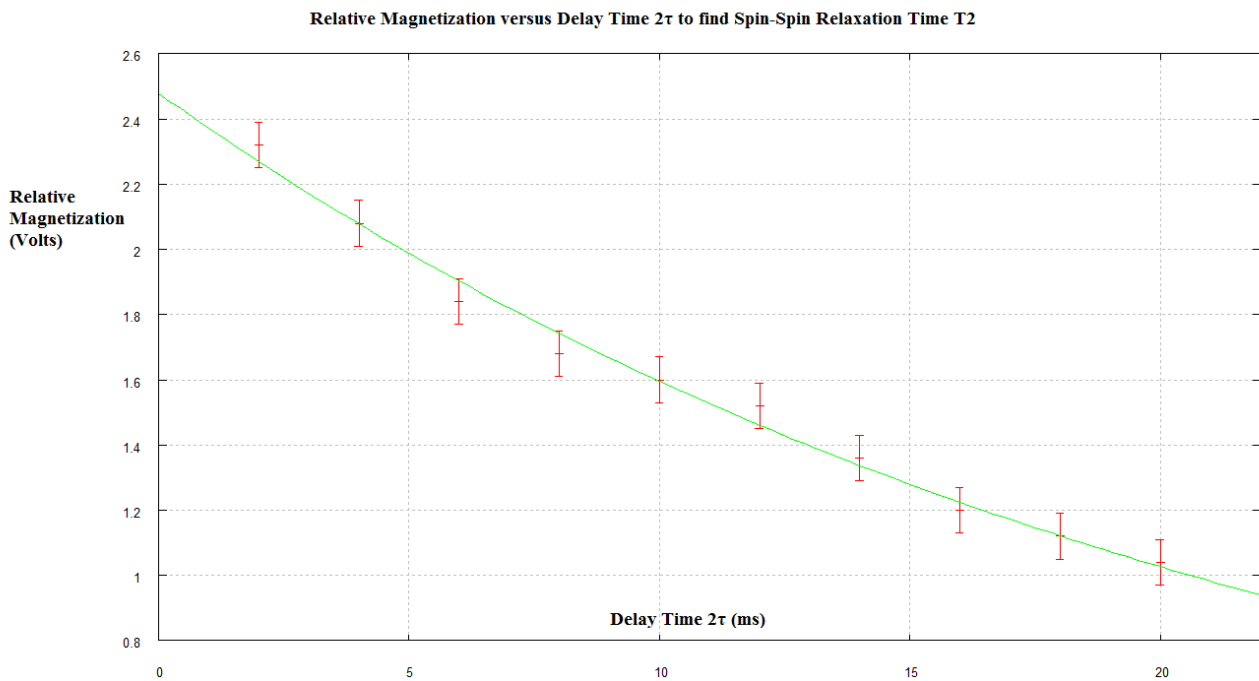


Figure 9

We plot $M(2\tau)$. Here the magnetization is proportional to the height of the spin-echo voltage height as seen on the oscilloscope. We extract the best fit and T_2 using Gnuplot's Marqardt algorithm.

$$\begin{aligned}
 T_2 &= 22.69 \pm 0.82 \text{ ms} \\
 \nu &= 8 \\
 \chi^2 &= 3.10136 \\
 \alpha &= 0.9278
 \end{aligned}$$

The confidence values were poor, although we believe that the spin-lattice time T_1 result is consistent with the χ^2 statistic. As for T_2 , we believe that a combination of noise and systematic error within the devices contributed too greatly to correlate the error. We cannot say that this measurement of T_1 was consistent with the statistic. It is possible that the source of these systematic errors was using the cursor function on the oscilloscope; placing the cursors on the edge of the noisy oscilloscope trace may not have been done consistently. A source of correlated error may have been the strong temperature response in the magnet; making measurements too slowly or too quickly may have changed the regime of linearity, or not have allowed the magnetization to equilibrate properly.

4 Summary

We determined the spin-lattice and spin-spin relaxation times for a sample of mineral oil to be 7.48 ± 0.39 ms and 22.69 ± 0.82 ms, respectively. Our confidence values on these measurements were poor, and we attributed this to correlated and systematic error. However, these measurements still serve as good order-of-magnitude estimations. Other experiments ([8], [9], [10]) suggest that T_1 is close to 20 ms and T_2 is close to 15 ms. In all, we made some good insights into the fundamentals of nuclear magnetic resonance.

5 Appendix

5.1 Acknowledgments

We would like to thank Alice Durant for her help with setting up the correct connections with which to observe free induction decay. We also thank professor David Smith for helping us view the raw mixer output in order to clearly see the beat frequencies.

References

- [1] Black, Eric D. "Nuclear Magnetic Resonance (NMR)." *California Institute of Technology* (2008): n. pag. Physics 77.
- [2] H. Y. Carr and E. M. Purcell, *Effects of diffusion on free precession in nuclear magnetic resonance experiments*, Phys. Rev. 94 (3), 630-638 (1954).
- [3] TeachSpin, Inc. "Pulsed Nuclear Magnetic Spectrometer". Lab handbook. Tri-Main Center 2495 Main Street, Suite 409 Buffalo, NY 14214-2153. November 1997. Web.
- [4] S. Meiboom, D. Gill: Rev of Sci Instruments 29, 6881 (1958) *The description of phase shift technique that opened up multiple pulse techniques to measuring very long T_2 's in liquids*. Web.
- [5] Griffiths, David J. *Introduction to Quantum Mechanics*. Upper Saddle River, NJ: Pearson Prentice Hall, 2005. Print.
- [6] Kibble, T. W. B. *Classical Mechanics*. Kibble. London: McGraw-Hill, 1973. Print.
- [7] Walker, John. Chi-Square Calculator. Fournilab Switzerland. John Walker, n.d. Web. 26 Feb. 2014.
<https://www.fournilab.ch/rpkp/experiments/analysis/chiCalc.html>.
- [8] Bianchini, L., and L. Coffey. "NMR Techniques Applied to Mineral Oil, Water, and Ethanol." (2010): n. pag. Physics Department, Brandeis University, MA, 02453. Web. 13 May 2014. <http://fraden.brandeis.edu/courses/phys39/phys39%20reports%20S2010/Bianchini-NMR.pdf>.
- [9] Mallen, David, Callie Fiedler, and Andy Vesci. "Analysis of Mineral Oil and Glycerin through PNMR." USD Department of Physics (2011): n. pag. 27 Mar. 2011. Web. 13 May 2014. <http://home.sandiego.edu/severn/p480w/NMRDJM.pdf>.
- [10] Patel, Birju. "Pulsed NMR." Department of Physics and Astronomy, The Johns Hopkins University, Baltimore, MD 21218 (2006): n. pag. 23 Oct. 2006. Web. http://www.pha.jhu.edu/courses/173.308/SampleLabs/Pulsed%20NMR_Birju%20Patel.pdf.